REPORT

A Recurrent Mutation in *CACNA1G* Alters Cav3.1 T-Type Calcium-Channel Conduction and Causes Autosomal-Dominant Cerebellar Ataxia

Marie Coutelier,[1,2,3,4,5,6,19] Iulia Blesneac,[7,8,19] Arnaud Monteil,[7,8] Marie-Lorraine Monin,[1,2,3,4,9] Kunie Ando,[1,2,3,4,10] Emeline Mundwiller,[4] Alfredo Brusco,[11,12] Isabelle Le Ber,[1,2,3,4,13] Mathieu Anheim,[14,15,16] Anna Castrioto,[17,18] Charles Duyckaerts,[1,2,3,4,10] Alexis Brice,[1,2,3,4,9] Alexandra Durr,[1,2,3,4,9] Philippe Lory,[7,8,20] and Giovanni Stevanin[1,2,3,4,6,9,20,*]

Hereditary cerebellar ataxias (CAs) are neurodegenerative disorders clinically characterized by a cerebellar syndrome, often accompanied by other neurological or non-neurological signs. All transmission modes have been described. In autosomal-dominant CA (ADCA), mutations in more than 30 genes are implicated, but the molecular diagnosis remains unknown in about 40% of cases. Implication of ion channels has long been an ongoing topic in the genetics of CA, and mutations in several channel genes have been recently connected to ADCA. In a large family affected by ADCA and mild pyramidal signs, we searched for the causative variant by combining linkage analysis and whole-exome sequencing. In *CACNA1G*, we identified a c.5144G>A mutation, causing an arginine-to-histidine (p.Arg1715His) change in the voltage sensor S4 segment of the T-type channel protein Cav3.1. Two out of 479 index subjects screened subsequently harbored the same mutation. We performed electrophysiological experiments in HEK293T cells to compare the properties of the p.Arg1715His and wild-type Cav3.1 channels. The current-voltage and the steady-state activation curves of the p.Arg1715His channel were shifted positively, whereas the inactivation curve had a higher slope factor. Computer modeling in deep cerebellar nuclei (DCN) neurons suggested that the mutation results in decreased neuronal excitability. Taken together, these data establish *CACNA1G*, which is highly expressed in the cerebellum, as a gene whose mutations can cause ADCA. This is consistent with the neuropathological examination, which showed severe Purkinje cell loss. Our study further extends our knowledge of the link between calcium channelopathies and CAs.

Hereditary cerebellar ataxias (CAs) are rare clinically and genetically heterogeneous neurodegenerative disorders.[1] They are characterized by a cerebellar syndrome, associated with other neurological or extra-neurological symptoms, and are inherited in all classical transmission modes. In autosomal-dominant CAs (ADCAs), the most frequent mutations are trinucleotide CAG-repeat expansions (present in seven genes),[2] coding for a polyglutamine stretch in the corresponding proteins. The second most frequent mutations are noncoding nucleotide expansions, followed by conventional mutations that have been described in more than 20 different genes. The causative variant remains unknown, however, in about 40% of individuals with ADCA.[2,3]

Over the last few years, next-generation sequencing has led to the identification of an increasing number of variants in many genes implicated in this pathology.[4] Mutations in multiple genes gathered in various common pathways, including channels, have highlighted their importance in the physiopathology of ADCAs. The first channel-coding gene to be involved in ADCAs was *CACNA1A* (MIM: 601011), encoding the P/Q-type voltage-gated calcium channel. Small polyglutamine expansions, loss-of-function mutations, or missense variants in this gene give rise to spinocerebellar ataxia type 6 (SCA6 [MIM: 183086]), episodic ataxia type 2 (MIM: 108500), or familial hemiplegic migraine type 1 (MIM: 141500).[5,6] Knockdown of the fibroblast growth factor gene *FGF14* (MIM: 601515), associated with SCA27 (MIM: 609307), reduces calcium currents in granule cells.[7] Mutations in other ion-channel genes, including the voltage-gated potassium-channel genes *KCNC3* (MIM: 176264; associated with SCA13 [MIM: 605259])[8] and *KCND3* (MIM: 605411; associated with SCA19 [MIM: 607346])[9,10] and

[1]INSERM U 1127, 75013 Paris, France; [2]Centre National de la Recherche Scientifique UMR 7225, 75013 Paris, France; [3]UMRS 1127, Université Pierre et Marie Curie (Paris 06), Sorbonne Universités, 75013 Paris, France; [4]Institut du Cerveau et de la Moelle Épinière, 75013 Paris, France; [5]Laboratory of Human Molecular Genetics, de Duve Institute, Université Catholique de Louvain, 1200 Brussels, Belgium; [6]Ecole Pratique des Hautes Etudes, 75014 Paris, France; [7]Centre National de la Recherche Scientifique UMR 5203 and INSERM U 1191, Institut de Génomique Fonctionnelle, Université de Montpellier, 34094 Montpellier, France; [8]LabEx "Ion Channel Science and Therapeutics," 34094 Montpellier, France; [9]Centre de Référence de Neurogénétique, Hôpital de la Pitié-Salpêtrière, Assistance Publique – Hôpitaux de Paris, 75013 Paris, France; [10]Laboratoire de Neuropathologie Escourolle, Hôpital de la Pitié-Salpêtrière, 75013 Paris, France; [11]Department of Medical Sciences, University of Turin, 10126 Turin, Italy; [12]Medical Genetics Unit, Città della Salute e della Scienza University Hospital, 10126 Turin, Italy; [13]Fédération des Maladies du Système Nerveux, Hôpital de la Pitié-Salpêtrière, Assistance Publique – Hôpitaux de Paris, 75013 Paris, France; [14]Département de Neurologie, Hôpital de Hautepierre, Centre Hospitalier Universitaire de Strasbourg, 67098 Strasbourg, France; [15]Institut de Génétique et de Biologie Moléculaire et Cellulaire, INSERM U 964, Centre National de la Recherche Scientifique UMR 7104, Université de Strasbourg, 67400 Illkirch, France; [16]Fédération de Médecine Translationnelle de Strasbourg, Université de Strasbourg, 67081 Strasbourg, France; [17]Unité Troubles du Mouvement, Pôle de Neurologie et Psychiatrie, Centre Hospitalier Universitaire de Grenoble, 38700 Grenoble, France; [18]Equipe Fonctions Cérébrales et Neuromodulation, Grenoble Institut des Neurosciences, INSERM U 836, Université Joseph Fourier, Commissariat à l'Énergie Atomique et aux Énergies Alternatives, Centre Hospitalier Universitaire de Grenoble, 38700 Grenoble, France
[19]These authors contributed equally to this work
[20]These authors contributed equally to this work
*Correspondence: giovanni.stevanin@upmc.fr
http://dx.doi.org/10.1016/j.ajhg.2015.09.007.

the ligand-gated ion-channel genes *ITPR1* (MIM: 147265; associated with SCA15 [MIM: 606658]) and *GRID2* (MIM: 602368),[1,11,12] have also been described. All these findings converge to emphasize the importance of ion balance, notably that of calcium ions, in cerebellar physiology.[13]

In this paper, we report three pedigrees in which ADCA segregates with a recurrent mutation inducing an amino acid change in the voltage sensor S4 segment of domain IV in Cav3.1, a T-type calcium channel protein encoded by *CACNA1G* (MIM: 604065). We present electrophysiological in vitro evidence that this p.Arg1715His variant (GenBank: NM_018896.4) alters the channel activity and thus shifts its steady-state activation curve toward more-positive values and changes its inactivation slope constant. In an in silico model of deep cerebellar nuclei (DCN) neurons, we established that decreased excitability is linked to these altered parameters. Altogether, we describe a monogenic disease linked to *CACNA1G* mutations; confirm the implication of Cav3.1 channels, which are highly expressed in Purkinje cells (PCs) and DCN neurons, in cerebellar physiology; and strengthen the gathering of evidence toward the prominence of calcium levels in CA pathophysiology.

Families AAD-SAL-233, AAD-GRE-319, and AAD-SAL-454, along with more than 500 other ADCA-affected pedigrees, were part of the Spastic Paraplegia and Ataxia (SPATAX) network cohort. Affected members and relatives were examined, and blood was taken after informed consent was obtained according to French legislation (Paris Necker ethics committee approval [RBM 01-29 and RBM 03-48] to A. Brice and A.D.). All clinical data are summarized in Table 1. The age of onset varied widely from 9 to 78 years; gait instability was the major manifesting symptom (in nine of ten individuals). Even after decades of progression, the disability and symptoms remained mild to moderate, indicating stable cerebellar involvement. Ocular signs, including saccadic pursuit, horizontal nystagmus, and transient diplopia, were often noted (in seven of ten individuals). Interestingly, pyramidal signs, ranging from reflex pyramidal syndrome to spastic gait, were present in five of ten individuals. Of note, depression was reported in three of ten individuals, and cognitive impairment was observed in two of ten individuals. When performed (in five individuals), MRI revealed predominantly vermian cerebellar atrophy and a normal pons (Figure S1).

Individual AAD-SAL-233-14 (III-9 in Figure 2) had provided written informed consent for brain donation. She died at age 83. The left brain hemisphere was examined, whereas samples from the right hemisphere were frozen and kept in the brain bank GIE Neuro-CEB (BioResource Research Impact Factor number BB-0033-00011) and declared to the Ministry of Research and Higher Education as required by French law. The brain bank has been officially authorized to provide samples to scientists (agreement AC-2007-5). Macroscopically, the cerebellar hemisphere and the vermis were, respectively, mildly and severely atrophic. The cerebral cortex appeared normal. Microscopically, the volume of the cerebellar white matter was reduced. Bergmann gliosis and empty baskets were evidence of PC loss, more prominent in the vermis. In the granular layer, the number of glomeruli was decreased. The cellular density was increased in the molecular layer, which appeared loosened (Figure 1). Unusually abundant polyglucosan bodies were observed in all cerebellar layers. The neuronal density in the dentate nucleus was normal, as was the density of myelinated axons in the hilus. There was no neuronal loss in the pontine nuclei. The number of neurons was reduced in the inferior olive, which appeared gliotic. The substantia nigra was normal.

Microscopic evidence of Alzheimer disease (AD [MIM: 104300]), including amyloid deposits in the cerebral cortex, the hippocampus, and the basal ganglia (Thal phase 3[14]), was also observed. Tau-positive neurofibrillary tangles, neuropil threads, and senile plaque coronae were seen in the entorhinal cortex and hippocampus. Associative cortices were mildly affected, and primary cortices were spared (Braak stage V[15]).

Polyglutamine and *C9orf72* (MIM: 614260) expansions had previously been excluded in all three index subjects via classic procedures. Linkage analysis was performed in family AAD-SAL-233 (Figure S2). Six major putative loci were detected, and maximal multipoint LOD scores ranged from +1.579 to +2.279. Whole-exome sequencing was performed in individuals AAD-SAL-233-15 (III-10 in Figure 2) and AAD-SAL-233-25 (IV-16 in Figure 2), and achieved 85%–87% 30× coverage, through enrichment capture using the SureSelect All Exon 50 Mb Kit (Agilent) and subsequent paired-end 75 bp massive parallel sequencing in a HiSeq 2000 sequencer (Illumina) (Table S1). Results were analyzed according to the following criteria: (1) the effect on the coding sequence of an established protein-coding gene, (2) the heterozygous state in affected individual 25 and absence from healthy individual 15, (3) the location within the non-excluded loci, and (4) a frequency under 0.1% in public databases (dbSNP137, NHLBI Exome Sequencing Project Exome Variant Server [EVS], and the Exome Aggregation Consortium [ExAC] Browser). Sanger validation and segregation analysis in all family members led to the identification of two candidate variants: a chr10: g.95372766G>A (c.284G>A; p.Arg95His) change (GenBank: NM_006204.3) in *PDE6C* (MIM: 600827) and a chr17: g.48694921G>A (c.5144G>A; p.Arg1715His) change (GenBank: NM_018896.4) in *CACNA1G* (MIM: 604065) (Figure 2; Table S2). Of note, *PDE6C* is much more tolerant to missense variations than *CACNA1G*, as estimated by Samocha et al.,[16] in that it has an observed-to-expected ratio of 236:261.5 (Z score = 0.77), whereas that of *CACNA1G* is 598:903.6 (Z score = 4.97).

We then screened ADCA index subjects for variants in *CACNA1G* (n = 479), *PDE6C*, and genes previously involved in ADCA (n = 384) by using amplicon-based panel-sequencing techniques, either with conventional

PCR amplification followed by GS Junior (Roche) sequencing (n = 95) or with microfluidic PCR amplification (Fluidigm Access Array) followed by MiSeq (Illumina) sequencing (n = 384) according to the manufacturers' protocols (Table S3). Results were analyzed according to the above-mentioned criteria. Two index subjects, AAD-GRE-319-12 (II-2 in Figure 2) and AAD-SAL-454-10 (III-1 in Figure 2), harbored the same *CACNA1G* c.5144G>A (p.Arg1715His) variant (GenBank: NM_018896.4). No recurrence of the above-mentioned *PDE6C* variant was observed. All detected *PDE6C* variants, reported in Table S4, were present in public databases.

No conventional mutations in genes previously involved in ADCA were found in AAD-GRE-319-12 (II-2 in Figure 2). AAD-SAL-454-10 (III-1 in Figure 2) also harbored a variant of unknown significance (American College of Medical Genetics and Genomics class 3) in *SPTBN2* (MIM: 604985; associated with SCA5 [MIM: 600224]), chr11: g.66455764G>A (c.6250G>A; p.Glu2084Lys) (GenBank: NM_006946.2), not located within the spectrin repeats, as previously described for all *SPTBN2* mutations.[17] It was reported at the heterozygous state in one individual in the EVS and one other individual in the ExAC Browser; almost all in silico prediction software predicted it to be tolerated (data not shown). No recurrence was observed in the other 383 index individuals tested.

Segregation of the *CACNA1G* c.5144G>A (p.Arg1715His) variant was established in two additional affected members of family AAD-GRE-319 (Figure 2). Other individuals harbored various *CACNA1G* variants (Table S5); however, their pathogenic effects could not be ascertained because of the lack of affected individuals for segregation studies, genetic elements suggesting deleterious effects, or electrophysiological anomalies (Table S6). Analysis of flanking variants identified two homozygous variants in the *CACNA1G* region (chr17: g.48652875A>G and chr17: g.48655493A>G) in individual AAD-SAL-454-10 (III-1 in Figure 2); these were absent in AAD-SAL-233-25 (IV-16 in Figure 2) and heterozygous in AAD-GRE-319-12 (II-2 in Figure 2), excluding a common founder effect for all three families.

We hence focused on the *CACNA1G* variant and not on the *PDE6C* one because of strict co-segregation with the disease, absence in public databases, more concordant pathogenicity prediction scores, slightly higher conservation scores (Table S2), lower tolerance to missense variation, extremely high expression in the cerebellum,[18–20] and the previous implication of *CACNA1A*, as well as other ion-channel genes, in cerebellar ataxias.

To study the effect of the p.Arg1715His variant on the electrophysiological characteristics of Cav3.1, we introduced the c.5144G>A mutation into the cDNA of the human Cav3.1 channel (isoform 5, UniProt: O43497-1[21]) by site-directed mutagenesis (QuikChange Lightning Site-Directed Mutagenesis Kit, Agilent Technologies). The WT and mutant cDNA constructs were then transfected into HEK239T cells, and macroscopic currents were recorded by whole-cell patch-clamp techniques. Figure 3A shows typical recordings of the calcium current generated by these channels. Several differences between the WT and the p.Arg1715His channel were observed. Notably, the aberrant channel exhibited a significant shift of the steady-state activation curve toward more-positive membrane-potential values. The half-activation potential changed from −47.20 ± 0.65 mV (n = 18) for the WT to −43.27 ± 0.73 mV (n = 16) for the p.Arg1715His channel ($p < 0.001$) (Figure 3B). The steady-state inactivation curve was also affected. Although the half-inactivation potential was unchanged (−70.91 ± 0.48 mV [n = 15] for the WT versus 70.68 ± 0.36 mV [n = 16] for p.Arg1715His), the slope factor was significantly higher for the aberrant channel (5.39 ± 0.11 mV [n = 16]) than for the WT (4.29 ± 0.07 mV [n = 15]) ($p < 0.0001$). As a consequence, the window current also shifted toward more-positive membrane potentials (Figure 3D). No significant change was observed in current density or other biophysical properties, such as activation and inactivation kinetics (Figures 3E and 3F), recovery from inactivation (Figure 3G), or deactivation kinetics (Figure 3H). T-type calcium channels, especially Cav3.1, are highly expressed in cerebellar neurons, including DCN neurons.[24] To determine the functional consequences that the p.Arg1715His change could have on firing, we used a DCN computer model[22] with both excitatory and inhibitory inputs from 150 mossy fibers and 450 PC synapses, respectively. Introduction of our experimental parameters for the steady-state activation and inactivation curves in this model revealed alteration of DCN firing properties. Notably, the p.Arg1715His change led to a diminution of the number of spikes per burst (four spikes compared to five for the WT; Figure 3I) and a delayed onset of burst firing, thus increasing the interval between the bursts (Figure 3I). These results suggest that the p.Arg1715His channel is responsible for a decrease in the neuronal excitability.

The Cav3.1 channel belongs to the family of voltage-gated calcium channels (VGCCs), a large family divided into two main subgroups: (1) low-voltage activated (LVA) VGCCs, also known as T-type channels, comprising the Cav3.1 (encoded by *CACNA1G*), Cav3.2, and Cav3.3 isoforms; and (2) high-voltage activated (HVA) VGCCs, further divided into L-type, P/Q-type, N-type, and R-type channels depending on their sensitivity to pharmacological agents.[25–27] VGCCs are major actors regulating the calcium entry into neurons and, in turn, play predominant roles in the regulation of membrane potential and also in the modulation of calcium signaling pathways, such as neurite outgrowth,[28] calcium-dependent gene transcription, neurotransmitter release, or regulation of enzymes such as protein kinase C,[27] whose gamma subunit is associated with spinocerebellar ataxia 14 (MIM: 05361) when mutations occur in *PRKCG* (MIM: 176980).[29] The variety of coexisting subtypes and isoforms allows the establishment of highly specific neuronal firing patterns.[27,30,31]

Table 1. Clinical Characteristics of Affected Individuals from Families AAD-SAL-233, AAD-GRE-319, and AAD-SAL-454

	Individual[a]														
	AAD-SAL-233-9 (III-3)	**AAD-SAL-233-14 (III-9)**	**AAD-SAL-233-20 (IV-4)**	**AAD-SAL-233-25 (IV-16)**		**AAD-SAL-233-45 (V-5)**		**AAD-SAL-233-46 (V-6)**	**AAD-GRE-319-12 (II-2)**			**AAD-GRE-319-13 (III-2)**	**AAD-GRE-319-14 (II-1)**	**AAD-SAL-454-10 (III-1)**	
Sex	female	female	male	female		female		female	female			male	female	male	
Age at onset (years)	20	68	41	9		19		18	37			40	78	30	
Symptoms at onset	vertigo	gait instability	gait instability	gait instability, vertigo		gait instability		gait instability	gait instability			gait instability	gait instability	gait instability	
Exam Results															
Exam year	1998	2012	1999	1999	2012	2001	2012	2009	1998	2012	2015	2015	2015	2000	2010
Age at exam (years)	73	82	43	42	53	28	39	32	57	69	74	51	79	37	47
Disease duration (years)	53	14	2	33	44	9	20	14	20	32	37	11	1	7	17
Disability score (SDFS)[b]	4/7	4/7	1/7	3/7	3/7	2/7	2/7	2/7	4/7	5/7	5/7	3/7	2/7	2/7	3/7
Cerebellar syndrome (SARA score)	moderate	yes	mild	mild	yes (20/40)	yes	mild (12.5/40)	mild	yes	yes (21/40)	yes (20.5/40)	mild (12/40)	mild (4/40)	yes	yes (12/40)
Cerebellar signs in ULs	yes	NA	no	no	yes	no	yes	yes	no	mild	mild	mild	no	no	yes
Dysarthria	severe	no	yes	yes	yes	no	yes	yes	yes	moderate	moderate	moderate	no	yes	yes
Ocular signs	limited upward gaze	NA	none	intermittent diplopia	hypometric saccades, square waves	saccadic pursuit	hypometric saccades	none	saccadic pursuit	saccadic pursuit	saccadic pursuit, diplopia, strabism	saccadic pursuit	saccadic pursuit	nystagmus	nystagmus
LL reflexes	+ (− ankle)	NA	++	++	++	+	+	N	+	N	+	N	N	N	N
Spastic gait	no	NA	mild	mild	mild	NA	no	no	NA	no	mild	no	no	no	no
UL reflexes	N	NA	++	++	++	N	+	N	+	N	+	N	N	N	N

(*Continued on next page*)

Table 1. *Continued*

	Individual[a]														
	AAD-SAL-233-9 (III-3)	**AAD-SAL-233-14 (III-9)**	**AAD-SAL-233-20 (IV-4)**	**AAD-SAL-233-25 (IV-16)**		**AAD-SAL-233-45 (V-5)**		**AAD-SAL-233-46 (V-6)**	**AAD-GRE-319-12 (II-2)**			**AAD-GRE-319-13 (III-2)**	**AAD-GRE-319-14 (II-1)**	**AAD-SAL-454-10 (III-1)**	
Babinski sign	no	NA	no	yes	yes	no	no	no	unilateral	no	no	no	no	yes	no
Decreased vibration sense at ankles	yes	NA	yes	no	no	no	yes	no	no	mild	mild	no	mild	no	yes
Urinary symptoms	urgency	NA	no	no	incontinence	no	no	no	no	no	urgency	no; erectile dysfunction	urgency	urgency	incontinence
Other signs	no	NA	no	no; myokymia orbicularis	postural UL and head tremor	no	no	no; myokymia orbicularis	scoliosis, swallowing difficulties	myokymia orbicularis	dysphagia, dysarthria	dysphagia, dysarthria	no	no	swallowing difficulties, psoriasis
Mood or cognitive impairment	no	Alzheimer disease	depression	depression	no	no	N	no	no	no	no	no	no	MMS 25/30, depression	no
Cerebral MRI	NA	NA	vermian atrophy less foliation of the hemispheres, N-acetyl-aspartate decrease	vermian atrophy	NA	vermian atrophy	NA	NA	vermian atrophy	NA	cerebellar atrophy (vermian++), white-matter hypersignals	NA	NA	vermian atrophy	cerebellar and brainstem hypoplasia and atrophy

Abbreviations are as follows: LL, lower limb; MMS, mini mental state; N, normal; NA, not available; SARA, scale for the assessment and rating of ataxia; SDFS, spinocerebellar degeneration functional score; UL, upper limb.
[a]Personal numbers are followed by pedigree numbers according to Figure 2.
[b]Scores are as follows: 0, no functional handicap; 1, no functional handicap but signs at examination; 2 (mild), ability to run; 3 (moderate), inability to run; 4 (severe), unlimited walking with one stick; 5, ability to walk with two sticks; 6, inability to walk and wheelchair requirement; 7, confinement to bed.

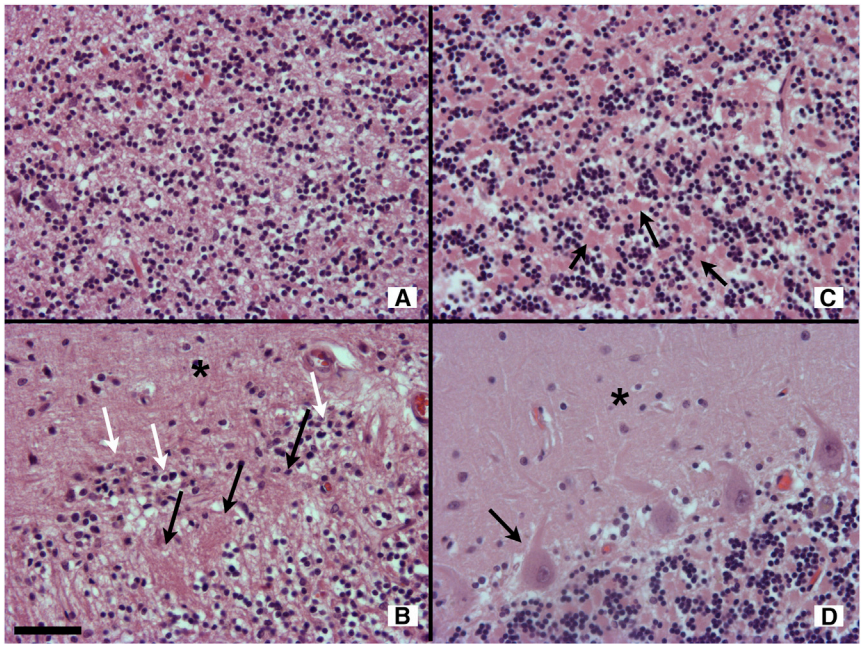

Figure 1. Neuropathological Examination of the Cerebellum
H&E staining in (A and B) individual AADSAL-233-14 (III-9 in Figure 2) and (C and D) a control individual.
(A and C) Granular layer of the cerebellum. The black arrows in (C) point to normal glomeruli; normal glomeruli cannot be identified in (A).
(B and D) Purkinje cell (PC) layer. Four normal PCs are visible in (D), and one of them is indicated by a black arrow; PC loss is severe in (B) such that only the processes of the basket cells are visible ("empty baskets," black arrows). Note the additional layer composed of Bergmann glia (white arrows). The asterisks in (B) and (D) indicate the molecular layer, which appears loosened in (B).

T-type Cav3 calcium channels differ from HVA-VGCCs by their ability to be activated and inactivated at low voltages (near the resting membrane potential), their faster recovery from inactivation, their slower deactivation, and a characteristic window current occurring in the range of the resting membrane potential of neurons.[32,33] In this respect, they act as pacemakers and excitability regulators,[27] allowing cells to be depolarized at the needed membrane potential for other channels' activation. This window current is also essential for the regulation of the intracellular calcium concentration.[34] In neurons, they have two essential behaviors: triggering a burst action potential after a low-threshold calcium spike[26,33] and rebound burst firing.[27,32,33] Of the three Cav3 isoforms, Cav3.1 is highly expressed in cerebellar neurons, as well as thalamic relay neurons,[18,20] where it plays a major role in the establishment of the slow (<1 Hz) sleep oscillations of non-rapid-eye-movement (REM) sleep.[32] Gain-of-function variants are thought to participate in the spike-and-wave discharges of thalamocortical neurons in absence epilepsy (MIM: 611942) through enhancement of thalamic oscillatory activities.[18,26,35,36]

In the cerebellum, a comprehensive study of Cav3 expression in neurons revealed that their specific patterns are correlated with various electrophysiological phenotypes.[31] In situ hybridization studies described *CACNA1G* mRNA in both PCs and DCN neurons.[20,37] In the DCN, Cav3.1 is predominantly expressed in a subset of large neurons exhibiting a strong ability to generate rebound burst firing after hyperpolarization.[31,38] Pharmacological evidence has confirmed that these rebound bursts are mediated by T-type calcium channels.[39] They appear to be physiologically relevant and consistent with a response to inhibitory input from PCs.[40] Their characteristics result from interplay between T-type channels and hyperpolarization-activated cyclic-nucleotide (HCN) channels.[24,40] In PCs, all three subtypes of Cav3 are expressed.[31] Cav3.1 was found at the cell body and at the synapse between parallel fibers (PFs) and PCs.[19] At this synapse, Cav3 channels interact with intermediate-conductance calcium-activated potassium (IKCa) channels to suppress the temporal summation of background excitatory postsynaptic potentials from PFs through afterhyperpolarization.[24,41] This is essential to allow the detection of sensory-relevant high-frequency inputs.[24,41] Finally, PC burst firing was shown to rely on P/Q-type calcium currents. In addition, T-type channels interact with large-conductance calcium-activated potassium (BK) channels to determine the firing rate, burst duration, and interburst interval.[42] Therefore, T-type channels, including Cav3 isoforms and specifically the Cav3.1 isoform, have major roles in the PF-PC-DCN signal processing. Of note, histologically, the neuronal density appeared normal in the dentate nucleus of our affected individual; marked PC loss was observed.

In mice, which show 93% Cav3.1 amino acid sequence identity with humans, no spontaneous *Cacna1g* mutations have been reported; however, several models have been generated. *Cacna1g*-null mice have normal growth, normal brain pathology, and no overt neurological phenotype;[43] in particular, they have no motor defects.[44] However, they present with a non-REM sleep disturbance,[45] are resistant to pharmacologically induced absence seizures,[43] show attenuated neuropathic pain,[46] and show bradycardia and slowed atrioventricular conduction.[47] The only cerebellar anomaly linked to *Cacna1g* inactivation was a loss of PCs in double-mutant mice lacking both Cav3.1 and the alpha-1 GABA-A receptor.[44] Compared to mice lacking only the GABA-A receptor, this mouse model showed exacerbated motor defects, including tremor. Conversely, transgenic mice overexpressing Cav3.1 showed spontaneous spike-and-wave discharges associated with behavioral arrest.[18]

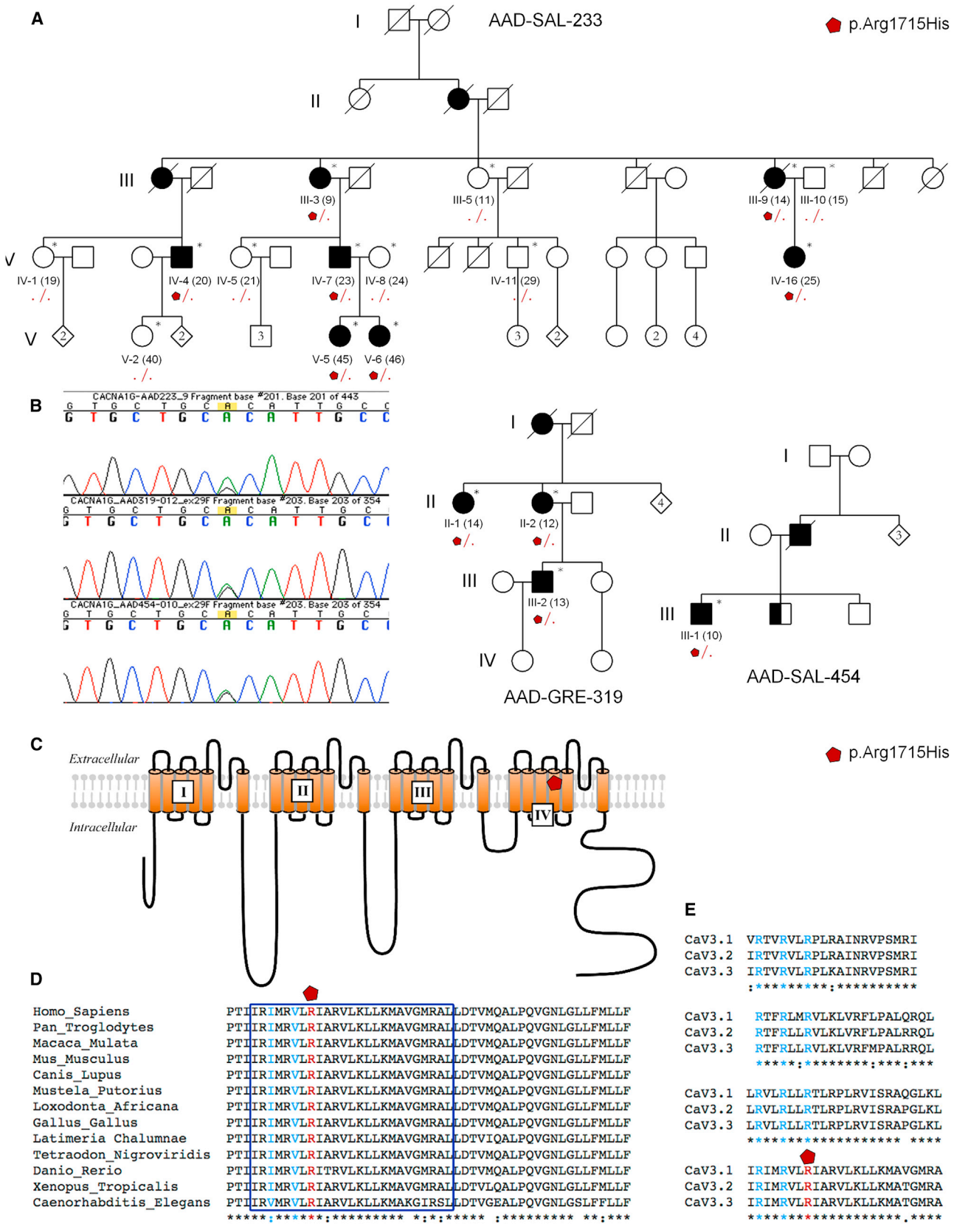

Figure 2. Segregation of the p.Arg1715His Change in ADCA-Affected Pedigrees and Alignment of Cav3.1 Orthologs and Paralogs
(A) Pedigrees of ADCA-affected families with the p.Arg1715His change. The numbers of affected individuals tested are as follows: six in AAD-SAL-233, three in AAD-GRE-319, and one in AAD-SAL-454. All affected, but no unaffected, individuals harbor the variant in the heterozygous state.

(legend continued on next page)

In human pathology, the role of T-type VGCCs has only been partially elucidated. In particular, no monogenic disease has clearly been linked to T-type channel gene mutations until now.[26,48] *CACNA1H* (MIM: 607904), encoding Cav3.2, is implicated in absence epilepsy[49–51] in that several mutations lead to increased activity of the channel.[52] However, in many cases, the variant induces susceptibility to seizures rather than having a monogenic causative effect.[26,50] As for *CACNA1G*, some variants have been described in idiopathic generalized epilepsy (MIM: 600669);[53] many, if not all, of them appear to be risk-factor variants and not causative mutations. *CACNA1G* was also associated with autism spectrum disorder (MIM: 209850), but the association was too weak to fully explain the odds ratio.[54] Finally, a large study on intellectual disability identified a homozygous *CACNA1G* frameshift variant in three siblings with associated cataracts but no reported cerebellar ataxia.[55]

Despite its predominant expression in PCs and DCN neurons, *CACNA1G* was never implicated by itself in cerebellar dysfunction. In three independent ADCA-affected families, we describe the recurrent p.Arg1715His variant in Cav3.1. There are strong genetic arguments in favor of the deleteriousness of this variant: (1) the concordance of all in silico pathogenicity predictions; (2) the variant's absence in all examined public databases (including more than 60,000 exomes); (3) amino acid conservation in all orthologs, paralogs, and S4 segments of all four domains of the protein; (4) the variant's location within a putatively linked locus (Figure S2); (5) the absence of pathogenic variants in all genes previously involved in ADCA; (6) the recurrence of the variant in three pedigrees in which a common founder effect was excluded; (7) perfect segregation in both pedigrees where it could be verified; and (8) the variant's location within a functionally important domain of the protein: the voltage sensor S4 segment. Importantly, in vitro studies showed that the variant alters electrophysiological characteristics of the channel, including activation at more-positive voltages, an increased slope factor of the steady-state inactivation curve, and consequently, a shift of the window current toward more-positive potentials. Minimal alterations in T-type VGCC properties can lead to marked alterations in firing dynamics.[56] Simulating the activity of a DCN neuron carrying either WT or p.Arg1715His Cav3.1 parameters also revealed a difference in burst firing, suggesting that the aberrant channel causes reduced neuronal excitability. Because the activity of DCN neurons and cerebellar PCs is involved in movement behavior,[57,58] our findings suggest that the p.Arg1715His change in Cav3.1 could affect motor control by altering DCN activity.

All together, these elements establish *CACNA1G* mutations as a monogenic cause of ADCA. The p.Arg1715His variant is recurrent and has a relatively high frequency of almost 0.6% in our cohort after exclusion of polyglutamine expansions (~0.3% of all ADCA). The other variants detected (Table S5) could be benign polymorphisms, variants that potentiate other ion-channel variants (such as loss-of-function *CACNA1A* mutations), or causative mutations. Further investigations will be needed to elucidate their effects.

Interestingly, the clinical picture in the families we describe does not include any form of epilepsy. Indeed, the p.Arg1715His variant induces a shift of activation toward positive voltages, whereas epilepsy-associated T-type channel variants are classically associated with a gain of function through faster activation, negative shift of steady-state activation and inactivation properties, or increased protein amounts.[26,52] In agreement with these observations, *CACNA1G*-null mice are resistant to induced seizures.[43] Expectedly, a positive shift in activation properties, as in our families, should be protective or have no effect.

It is of note that, in family AAD-SAL-233, individual 14 (III-9 in Figure 2) presented with both clinical signs and pathological characteristics of AD. Another family member presented with ataxia and Alzheimer-type dementia, but no DNA was available for sequencing, and the brain was not available. *CACNA1G* downregulation and Cav3.1 inhibition were recently correlated with altered APP (amyloid precursor protein) processing and, consequently, the occurrence of AD markers in microarrays of human tissue, mice, and cellular models.[59] We could not determine whether the p.Arg1715His change is related to AD in this individual. Nevertheless, the co-occurrence of AD at 83 years of age is not unexpected.

It is interesting to note that the variant we describe, p.Arg1715His, modifies a highly conserved arginine in the S4 segment in domain IV of the channel. All T-type channels share a common general membrane topology with four domain repeats, each including six transmembrane segments (S1–S6). S4 segments, through their positive arginine residues, are considered the voltage-sensing elements, and their alteration is expected to affect the voltage dependency of the channel. A systematic mutagenesis study in Cav3.1 showed that loss of the outermost arginine residues in the voltage sensor S4 segment of domain IV affects the steady-state inactivation curve.[60] Our results establish that Arg1715, the third outermost arginine in domain IV (R3), also plays a role in Cav3.1 gating by shifting the steady-state activation curve and changing the

(B) Chromatograms show the mutation in individuals AAD-SAL-233-9 (III-3), AAD-GRE-319-12 (II-2), and AAD-SAL-454-10 (III-1).
(C) A schematic representation of Cav3.1 shows its organization in four domains, each containing six transmembrane segments; segment S4 contains many positively charged amino acids, such as arginine, and is therefore the voltage sensor. The p.Arg1715His change is located in segment S4 of domain IV.
(D and E) Alignment of orthologs (D) and paralogs (E) shows that the arginine residues in Cav3.1 are very highly conserved across all species, T-type channels, and domains.

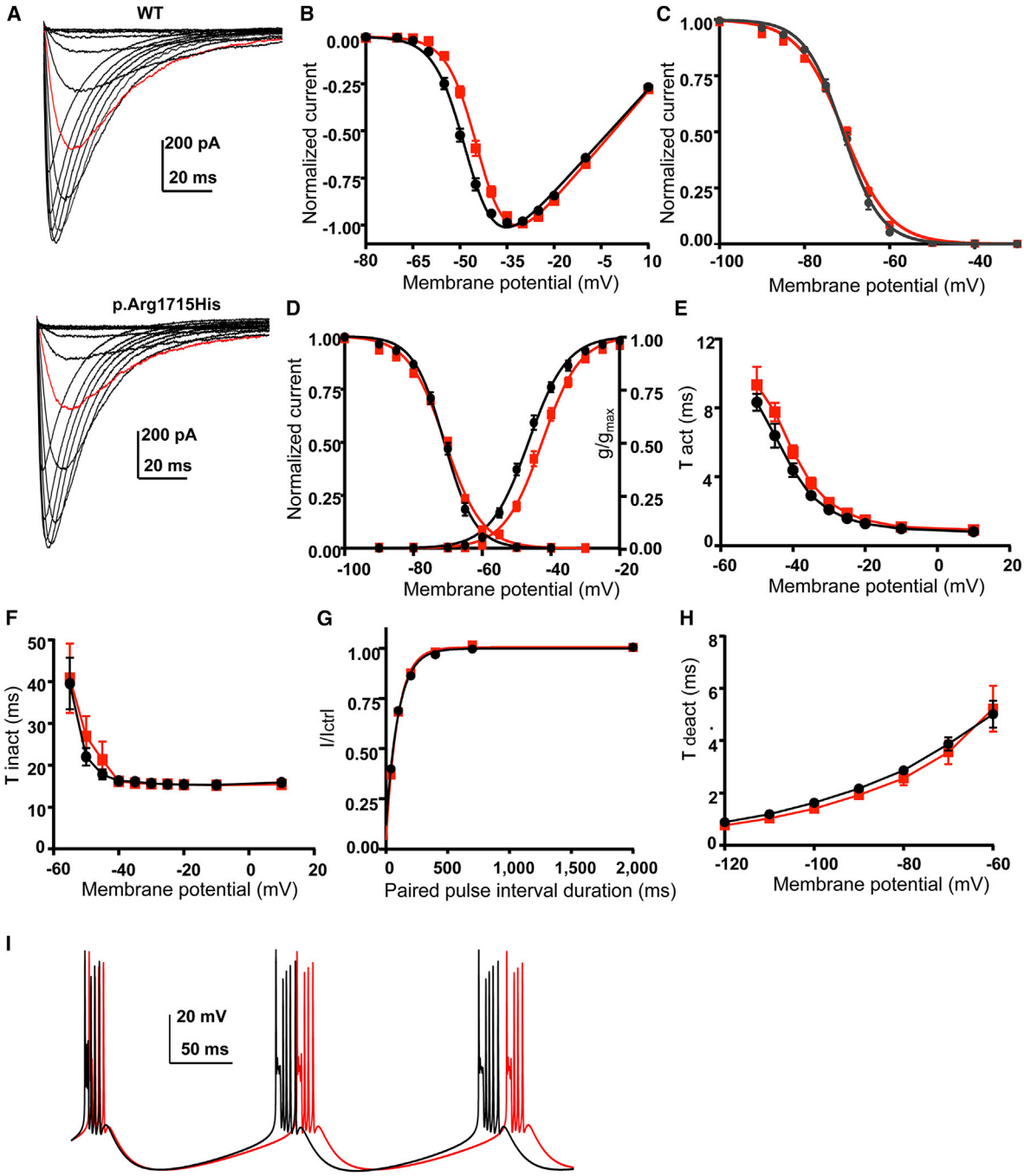

Figure 3. Electrophysiological Analysis of WT and p.Arg1715His Cav3.1 Calcium Channels

(A) Current traces obtained with wild-type (WT) and p.Arg1715His channels at various membrane potentials (−90, −80, −70, −65, −60, −55, −50, −45, −40, −35, −30, −25, and −20 mV) and from a holding potential of −100 mV. Notice the red trace (−50 mV), which shows a smaller current for the p.Arg1715His channel (36% of the maximum current) than for the WT (54%)

(B) Averaged current-voltage relationships from traces in (A). The normalized conductance-voltage curve was fitted with a Boltzmann equation: $I/I_{max} = G_{max}(V_m - E_{rev})/(1 + \exp(V_{1/2} - V_m)/k)$.

(C) Steady-state inactivation curves. The curves were fitted with $I/I_{max} = 1/(1 + \exp(V_m - V_{1/2})/k)$.

(D) Availability of calcium currents (mean steady-state activation and inactivation curves). The steady-state activation curves were fitted with a Boltzmann equation, $G/G_{max} = 1/(1 + \exp(V_{1/2} - V_m)/k)$, where G was calculated as follows: $G = I/(V_m - E_{rev})$.

(E and F) Time constant of inactivation (τ inact) and activation (τ act) kinetics. Fitting the traces showed in (A) with a double exponential function produced the values shown.

(G) Recovery from short-term inactivation according to a two-paired-pulse protocol.

(H) Deactivation kinetics (τ deact).

(I) DCN neuron firing was simulated with the steady-state activation and inactivation values obtained for the WT (black) and the p.Arg1715His (red) channels. The DCN model used was developed by Luthman et al.[22] with the NEURON simulation environment

(legend continued on next page)

slope of the steady-state inactivation curve. This is consistent with the observation, in Cav3.2, that the equivalent arginine-to-histidine change (R3) also induces a positive shift in the steady-state activation curve of the protein at pH 6.5[61]; this would be expected from eliminating one of the arginines in segment S4.

In conclusion, we report three ADCA-affected families in whom a common variant affecting an arginine residue in the voltage sensor S4 segment of domain IV in Cav3.1 segregates with the disease. Genetic and electrophysiological evidence support the pathogenicity of this variant. These results underscore the prominent role of Cav3.1-mediated calcium currents in cerebellar physiology, whereas previous reports on dysfunctions of this channel have focused on thalamocortical relay neurons. We describe a monogenic disease caused by alteration of T-type currents. Our results also underscore the important role played by the S4 segment of domain IV in the gating properties of Cav3.1. Finally, we provide further evidence of the importance of ion-channel function in the physiopathology of cerebellar ataxia and, in particular, of calcium-related pathways.

Supplemental Data

Supplemental Data include three figures and six tables and can be found with this article online at http://dx.doi.org/10.1016/j.ajhg.2015.09.007.

Acknowledgments

The authors thank the families for their contribution, as well as the DNA and cell bank of the Institut du Cerveau et de la Moelle Épinière (ICM) and the brain bank GIE NeuroCEB (funded by Institut Hospitalo-Universitaire A-ICM and by private foundations France Alzheimer, France Parkinson, Association de Recherche sur la Sclérose en Plaques, and Connaitre les Syndromes Cérébelleux). The authors also thank Célia Gautier for helping with this study, as well as Drs. Stephan Klebe, Chantal Tallaksen, and Imed Féki for examining subjects. M.C. was the recipient of a fellowship from the Fond National de la Recherche Scientifique (aspirant FNRS). This work received financial support from the French National Agency for Research (ANR; to G.S.), the French Ministry of Health PHRC 2009 program (AOM 09178 to A.D.), the European Union (Omics call: NeurOmics; to A. Brice and A.D.), the Verum Foundation (to A. Brice and G.S.), the Fondation Roger de Spoelberch (to A. Brice), the Association Connaitre les Syndromes Cérébelleux (to G.S.), the program Investissements d'Avenir (ANR-10-IAIHU-06; to the ICM), and the Associazione Italiana Sindromi Atassiche (to A. Brusco).

Received: June 25, 2015
Accepted: September 18, 2015
Published: October 8, 2015

Web Resources

The URLs for data presented herein are as follows:

dbSNP137, http://www.ncbi.nlm.nih.gov/projects/SNP
Exome Aggregation Consortium (ExAC) Browser, http://exac.broadinstitute.org
NEURON simulation environment, https://www.neuron.yale.edu/neuron/
NHLBI Exome Sequencing Project (ESP) Exome Variant Server, http://evs.gs.washington.edu/EVS/
OMIM, http://www.omim.org
Scale for the Assessment and Rating of Ataxia, http://www.ataxia-study-group.net/html/about/ataxiascales/sara/SARA.pdf
SPATAX Network, https://spatax.wordpress.com/

References

1. Matilla-Dueñas, A., Ashizawa, T., Brice, A., Magri, S., McFarland, K.N., Pandolfo, M., Pulst, S.M., Riess, O., Rubinsztein, D.C., Schmidt, J., et al. (2014). Consensus paper: pathological mechanisms underlying neurodegeneration in spinocerebellar ataxias. Cerebellum *13*, 269–302.
2. Durr, A. (2010). Autosomal dominant cerebellar ataxias: polyglutamine expansions and beyond. Lancet Neurol. *9*, 885–894.
3. Hersheson, J., Haworth, A., and Houlden, H. (2012). The inherited ataxias: genetic heterogeneity, mutation databases, and future directions in research and clinical diagnostics. Hum. Mutat. *33*, 1324–1332.
4. Coutelier, M., Stevanin, G., and Brice, A. (2015). Genetic landscape remodelling in spinocerebellar ataxias: the influence of next-generation sequencing. J. Neurol. http://dx.doi.org/10.1007/s00415-015-7725-4.
5. Giunti, P., Mantuano, E., Frontali, M., and Veneziano, L. (2015). Molecular mechanism of Spinocerebellar Ataxia type 6: glutamine repeat disorder, channelopathy and transcriptional dysregulation. The multifaceted aspects of a single mutation. Front. Cell. Neurosci. *9*, 36.
6. Rajakulendran, S., Kaski, D., and Hanna, M.G. (2012). Neuronal P/Q-type calcium channel dysfunction in inherited disorders of the CNS. Nat. Rev. Neurol. *8*, 86–96.
7. Yan, H., Pablo, J.L., and Pitt, G.S. (2013). FGF14 regulates presynaptic Ca2+ channels and synaptic transmission. Cell Rep. *4*, 66–75.
8. Waters, M.F., Minassian, N.A., Stevanin, G., Figueroa, K.P., Bannister, J.P., Nolte, D., Mock, A.F., Evidente, V.G., Fee, D.B., Müller, U., et al. (2006). Mutations in voltage-gated

(see Web Resources) on the basis of the model originally implemented in GENESIS by Steuber et al.[23] The NaP, HCN, and CaLVA conductances were changed to match the "Neuron 1" model described by Steuber et al.[23]
In the above-mentioned equations, $V_{1/2}$ represents either the half-activation potential (steady-state activation curve) or the half-inactivation potential (steady-state inactivation curve). Other parameters are V_m, membrane potential; E_{rev}, reversal potential; k, slope factor; G, conductance; G_{max}, maximum conductance; I, current at a given V_m; and I_{max}, maximum current. The extracellular solution contained 135 mM NaCl, 20 mM TEACl, 2 mM $CaCl_2$, 1 mM $MgCl_2$, and 10 mM HEPES (pH adjusted to 7.44 with KOH). Patch pipettes were filled with an internal solution (140 mM CsCl, 10 mM EGTA, 3 mM $CaCl_2$, 10 mM HEPES, 3 mM Mg-ATP, and 0.6 mM GTP [pH adjusted to 7.25 with KOH]) and had a typical resistance of 2–3 MΩ. In (B)–(H), WT values are represented by black circles, and p.Arg1715His values are represented by red squares. Data represent the mean ± SEM.

potassium channel KCNC3 cause degenerative and developmental central nervous system phenotypes. Nat. Genet. *38*, 447–451.
9. Duarri, A., Jezierska, J., Fokkens, M., Meijer, M., Schelhaas, H.J., den Dunnen, W.F., van Dijk, F., Verschuuren-Bemelmans, C., Hageman, G., van de Vlies, P., et al. (2012). Mutations in potassium channel kcnd3 cause spinocerebellar ataxia type 19. Ann. Neurol. *72*, 870–880.
10. Lee, Y.C., Durr, A., Majczenko, K., Huang, Y.H., Liu, Y.C., Lien, C.C., Tsai, P.C., Ichikawa, Y., Goto, J., Monin, M.L., et al. (2012). Mutations in KCND3 cause spinocerebellar ataxia type 22. Ann. Neurol. *72*, 859–869.
11. Hills, L.B., Masri, A., Konno, K., Kakegawa, W., Lam, A.T., Lim-Melia, E., Chandy, N., Hill, R.S., Partlow, J.N., Al-Saffar, M., et al. (2013). Deletions in GRID2 lead to a recessive syndrome of cerebellar ataxia and tonic upgaze in humans. Neurology *81*, 1378–1386.
12. Coutelier, M., Burglen, L., Mundwiller, E., Abada-Bendib, M., Rodriguez, D., Chantot-Bastaraud, S., Rougeot, C., Cournelle, M.A., Milh, M., Toutain, A., et al. (2015). GRID2 mutations span from congenital to mild adult-onset cerebellar ataxia. Neurology *84*, 1751–1759.
13. Chopra, R., and Shakkottai, V.G. (2014). Translating cerebellar Purkinje neuron physiology to progress in dominantly inherited ataxia. Future Neurol. *9*, 187–196.
14. Thal, D.R., Rüb, U., Orantes, M., and Braak, H. (2002). Phases of A beta-deposition in the human brain and its relevance for the development of AD. Neurology *58*, 1791–1800.
15. Braak, H., and Braak, E. (1991). Neuropathological stageing of Alzheimer-related changes. Acta Neuropathol. *82*, 239–259.
16. Samocha, K.E., Robinson, E.B., Sanders, S.J., Stevens, C., Sabo, A., McGrath, L.M., Kosmicki, J.A., Rehnström, K., Mallick, S., Kirby, A., et al. (2014). A framework for the interpretation of de novo mutation in human disease. Nat. Genet. *46*, 944–950.
17. Ikeda, Y., Dick, K.A., Weatherspoon, M.R., Gincel, D., Armbrust, K.R., Dalton, J.C., Stevanin, G., Dürr, A., Zühlke, C., Bürk, K., et al. (2006). Spectrin mutations cause spinocerebellar ataxia type 5. Nat. Genet. *38*, 184–190.
18. Ernst, W.L., Zhang, Y., Yoo, J.W., Ernst, S.J., and Noebels, J.L. (2009). Genetic enhancement of thalamocortical network activity by elevating alpha 1g-mediated low-voltage-activated calcium current induces pure absence epilepsy. J. Neurosci. *29*, 1615–1625.
19. Ly, R., Bouvier, G., Schonewille, M., Arabo, A., Rondi-Reig, L., Léna, C., Casado, M., De Zeeuw, C.I., and Feltz, A. (2013). T-type channel blockade impairs long-term potentiation at the parallel fiber-Purkinje cell synapse and cerebellar learning. Proc. Natl. Acad. Sci. USA *110*, 20302–20307.
20. Talley, E.M., Cribbs, L.L., Lee, J.H., Daud, A., Perez-Reyes, E., and Bayliss, D.A. (1999). Differential distribution of three members of a gene family encoding low voltage-activated (T-type) calcium channels. J. Neurosci. *19*, 1895–1911.
21. Monteil, A., Chemin, J., Bourinet, E., Mennessier, G., Lory, P., and Nargeot, J. (2000). Molecular and functional properties of the human alpha(1G) subunit that forms T-type calcium channels. J. Biol. Chem. *275*, 6090–6100.
22. Luthman, J., Hoebeek, F.E., Maex, R., Davey, N., Adams, R., De Zeeuw, C.I., and Steuber, V. (2011). STD-dependent and independent encoding of input irregularity as spike rate in a computational model of a cerebellar nucleus neuron. Cerebellum *10*, 667–682.
23. Steuber, V., Schultheiss, N.W., Silver, R.A., De Schutter, E., and Jaeger, D. (2011). Determinants of synaptic integration and heterogeneity in rebound firing explored with data-driven models of deep cerebellar nucleus cells. J. Comput. Neurosci. *30*, 633–658.
24. Engbers, J.D., Anderson, D., Zamponi, G.W., and Turner, R.W. (2013). Signal processing by T-type calcium channel interactions in the cerebellum. Front. Cell. Neurosci. *7*, 230.
25. Perez-Reyes, E. (2006). Molecular characterization of T-type calcium channels. Cell Calcium *40*, 89–96.
26. Cain, S.M., and Snutch, T.P. (2011). Voltage-gated calcium channels and disease. Biofactors *37*, 197–205.
27. Simms, B.A., and Zamponi, G.W. (2014). Neuronal voltage-gated calcium channels: structure, function, and dysfunction. Neuron *82*, 24–45.
28. Hamid, J., Peloquin, J.B., Monteil, A., and Zamponi, G.W. (2006). Determinants of the differential gating properties of Cav3.1 and Cav3.3 T-type channels: a role of domain IV? Neuroscience *143*, 717–728.
29. Chen, D.H., Brkanac, Z., Verlinde, C.L., Tan, X.J., Bylenok, L., Nochlin, D., Matsushita, M., Lipe, H., Wolff, J., Fernandez, M., et al. (2003). Missense mutations in the regulatory domain of PKC gamma: a new mechanism for dominant nonepisodic cerebellar ataxia. Am. J. Hum. Genet. *72*, 839–849.
30. Chemin, J., Monteil, A., Perez-Reyes, E., Bourinet, E., Nargeot, J., and Lory, P. (2002). Specific contribution of human T-type calcium channel isotypes (alpha(1G), alpha(1H) and alpha(1I)) to neuronal excitability. J. Physiol. *540*, 3–14.
31. Molineux, M.L., McRory, J.E., McKay, B.E., Hamid, J., Mehaffey, W.H., Rehak, R., Snutch, T.P., Zamponi, G.W., and Turner, R.W. (2006). Specific T-type calcium channel isoforms are associated with distinct burst phenotypes in deep cerebellar nuclear neurons. Proc. Natl. Acad. Sci. USA *103*, 5555–5560.
32. Crunelli, V., Tóth, T.I., Cope, D.W., Blethyn, K., and Hughes, S.W. (2005). The 'window' T-type calcium current in brain dynamics of different behavioural states. J. Physiol. *562*, 121–129.
33. Perez-Reyes, E. (2003). Molecular physiology of low-voltage-activated t-type calcium channels. Physiol. Rev. *83*, 117–161.
34. Chemin, J., Monteil, A., Briquaire, C., Richard, S., Perez-Reyes, E., Nargeot, J., and Lory, P. (2000). Overexpression of T-type calcium channels in HEK-293 cells increases intracellular calcium without affecting cellular proliferation. FEBS Lett. *478*, 166–172.
35. Shin, H.S., Cheong, E.J., Choi, S., Lee, J., and Na, H.S. (2008). T-type Ca2+ channels as therapeutic targets in the nervous system. Curr. Opin. Pharmacol. *8*, 33–41.
36. Yalçın, O. (2012). Genes and molecular mechanisms involved in the epileptogenesis of idiopathic absence epilepsies. Seizure *21*, 79–86.
37. Craig, P.J., Beattie, R.E., Folly, E.A., Banerjee, M.D., Reeves, M.B., Priestley, J.V., Carney, S.L., Sher, E., Perez-Reyes, E., and Volsen, S.G. (1999). Distribution of the voltage-dependent calcium channel alpha1G subunit mRNA and protein throughout the mature rat brain. Eur. J. Neurosci. *11*, 2949–2964.
38. Molineux, M.L., Mehaffey, W.H., Tadayonnejad, R., Anderson, D., Tennent, A.F., and Turner, R.W. (2008). Ionic factors governing rebound burst phenotype in rat deep cerebellar neurons. J. Neurophysiol. *100*, 2684–2701.
39. Alviña, K., Ellis-Davies, G., and Khodakhah, K. (2009). T-type calcium channels mediate rebound firing in intact deep cerebellar neurons. Neuroscience *158*, 635–641.

40. Engbers, J.D., Anderson, D., Tadayonnejad, R., Mehaffey, W.H., Molineux, M.L., and Turner, R.W. (2011). Distinct roles for I(T) and I(H) in controlling the frequency and timing of rebound spike responses. J. Physiol. *589*, 5391–5413.
41. Engbers, J.D., Anderson, D., Asmara, H., Rehak, R., Mehaffey, W.H., Hameed, S., McKay, B.E., Kruskic, M., Zamponi, G.W., and Turner, R.W. (2012). Intermediate conductance calcium-activated potassium channels modulate summation of parallel fiber input in cerebellar Purkinje cells. Proc. Natl. Acad. Sci. USA *109*, 2601–2606.
42. Womack, M.D., and Khodakhah, K. (2004). Dendritic control of spontaneous bursting in cerebellar Purkinje cells. J. Neurosci. *24*, 3511–3521.
43. Kim, D., Song, I., Keum, S., Lee, T., Jeong, M.J., Kim, S.S., McEnery, M.W., and Shin, H.S. (2001). Lack of the burst firing of thalamocortical relay neurons and resistance to absence seizures in mice lacking alpha(1G) T-type Ca(2+) channels. Neuron *31*, 35–45.
44. Chang, K.Y., Park, Y.G., Park, H.Y., Homanics, G.E., Kim, J., and Kim, D. (2011). Lack of CaV3.1 channels causes severe motor coordination defects and an age-dependent cerebellar atrophy in a genetic model of essential tremor. Biochem. Biophys. Res. Commun. *410*, 19–23.
45. Lee, J., Kim, D., and Shin, H.S. (2004). Lack of delta waves and sleep disturbances during non-rapid eye movement sleep in mice lacking alpha1G-subunit of T-type calcium channels. Proc. Natl. Acad. Sci. USA *101*, 18195–18199.
46. Na, H.S., Choi, S., Kim, J., Park, J., and Shin, H.S. (2008). Attenuated neuropathic pain in Cav3.1 null mice. Mol. Cells *25*, 242–246.
47. Mangoni, M.E., Traboulsie, A., Leoni, A.L., Couette, B., Marger, L., Le Quang, K., Kupfer, E., Cohen-Solal, A., Vilar, J., Shin, H.S., et al. (2006). Bradycardia and slowing of the atrioventricular conduction in mice lacking CaV3.1/alpha1G T-type calcium channels. Circ. Res. *98*, 1422–1430.
48. Bidaud, I., and Lory, P. (2011). Hallmarks of the channelopathies associated with L-type calcium channels: a focus on the Timothy mutations in Ca(v)1.2 channels. Biochimie *93*, 2080–2086.
49. Chen, Y., Lu, J., Pan, H., Zhang, Y., Wu, H., Xu, K., Liu, X., Jiang, Y., Bao, X., Yao, Z., et al. (2003). Association between genetic variation of CACNA1H and childhood absence epilepsy. Ann. Neurol. *54*, 239–243.
50. Heron, S.E., Phillips, H.A., Mulley, J.C., Mazarib, A., Neufeld, M.Y., Berkovic, S.F., and Scheffer, I.E. (2004). Genetic variation of CACNA1H in idiopathic generalized epilepsy. Ann. Neurol. *55*, 595–596.
51. Khosravani, H., Altier, C., Simms, B., Hamming, K.S., Snutch, T.P., Mezeyova, J., McRory, J.E., and Zamponi, G.W. (2004). Gating effects of mutations in the Cav3.2 T-type calcium channel associated with childhood absence epilepsy. J. Biol. Chem. *279*, 9681–9684.
52. Eckle, V.S., Shcheglovitov, A., Vitko, I., Dey, D., Yap, C.C., Winckler, B., and Perez-Reyes, E. (2014). Mechanisms by which a CACNA1H mutation in epilepsy patients increases seizure susceptibility. J. Physiol. *592*, 795–809.
53. Singh, B., Monteil, A., Bidaud, I., Sugimoto, Y., Suzuki, T., Hamano, S., Oguni, H., Osawa, M., Alonso, M.E., Delgado-Escueta, A.V., et al. (2007). Mutational analysis of CACNA1G in idiopathic generalized epilepsy. Mutation in brief #962. Online. Hum. Mutat. *28*, 524–525.
54. Strom, S.P., Stone, J.L., Ten Bosch, J.R., Merriman, B., Cantor, R.M., Geschwind, D.H., and Nelson, S.F. (2010). High-density SNP association study of the 17q21 chromosomal region linked to autism identifies CACNA1G as a novel candidate gene. Mol. Psychiatry *15*, 996–1005.
55. Najmabadi, H., Hu, H., Garshasbi, M., Zemojtel, T., Abedini, S.S., Chen, W., Hosseini, M., Behjati, F., Haas, S., Jamali, P., et al. (2011). Deep sequencing reveals 50 novel genes for recessive cognitive disorders. Nature *478*, 57–63.
56. Tscherter, A., David, F., Ivanova, T., Deleuze, C., Renger, J.J., Uebele, V.N., Shin, H.S., Bal, T., Leresche, N., and Lambert, R.C. (2011). Minimal alterations in T-type calcium channel gating markedly modify physiological firing dynamics. J. Physiol. *589*, 1707–1724.
57. Heiney, S.A., Wohl, M.P., Chettih, S.N., Ruffolo, L.I., and Medina, J.F. (2014). Cerebellar-dependent expression of motor learning during eyeblink conditioning in head-fixed mice. J. Neurosci. *34*, 14845–14853.
58. Witter, L., Canto, C.B., Hoogland, T.M., de Gruijl, J.R., and De Zeeuw, C.I. (2013). Strength and timing of motor responses mediated by rebound firing in the cerebellar nuclei after Purkinje cell activation. Front. Neural Circuits *7*, 133.
59. Rice, R.A., Berchtold, N.C., Cotman, C.W., and Green, K.N. (2014). Age-related downregulation of the CaV3.1 T-type calcium channel as a mediator of amyloid beta production. Neurobiol. Aging *35*, 1002–1011.
60. Kurejová, M., Lacinová, L., Pavlovicová, M., Eschbach, M., and Klugbauer, N. (2007). The effect of the outermost basic residues in the S4 segments of the Ca(V)3.1 T-type calcium channel on channel gating. Pflugers Arch. *455*, 527–539.
61. Lam, A.D., Chikina, M.D., McNulty, M.M., Glaaser, I.W., and Hanck, D.A. (2005). Role of Domain IV/S4 outermost arginines in gating of T-type calcium channels. Pflugers Arch. *451*, 349–361.